Intelligent Recognition of Acoustic and Vibration Threats for Security Breach Detection, Close Proximity Danger Identification, and Perimeter Protection[1]

Alireza A. Dibazar, Ali Yousefi, Hyung O. Park, Bing Lu, Sageev George, and Theodore W. Berger

ABSTRACT:

The protection of perimeters in national, agricultural, airport, prison, and military sites, and residential areas against dangerous approaching human and vehicles when using human agents to provide security is expensive or unsafe. Because of this, acoustic/vibration signature identification of approaching human and vehicles threats has attracted increased attention. This paper addresses the development and deployment of three types of acoustic and vibration based smart sensors to identify and report sequential approaching threats prior to the intrusion. More specifically, we have developed: a) acoustic based long range sensor with which vehicles' engine sound and type can be identified, b) vibration based seismic analyzer which discriminates between human footsteps and other seismic events such as those caused by animals, and c) fence breaching vibration sensor which can detect intentional disturbances on the fence and discriminate between climb, kick, rattle, and lean. All of these sensors were designed with several issues in mind, namely, optimized low power usage, a low number of false positives, small size, secure radio communication, and milspec. The developed vibration based system was installed in an airport with unprotected shore lines in the vicinity of taxi- and run-ways. The system reported an average of less than two false positives per week and zero false negative for the duration of forty-five days. Six fence sensors were installed on the terminal area and end-of-runway chain-link fences where there was possibility of intentional fence climbing. The fence sensors reported no false positives for the duration of forty-five days which included several days of seasonal storms.

INTRODUCTION

The increasing emphasis on perimeter protection of national assets, both at home and abroad, has spurred the development of technologies that can detect potential threats, such as humans or approaching vehicles. One area of interest is the combination of several different sensors, each with their own distinct modalities and detection ranges, to create a versatile and robust system. We propose a system that would be based on three security sensors which have been demonstrated to provide detection and classification of security threats. These sensor types are acoustic, seismic, and vibration sensors.

The "Smart Fence" system based on these sensors would be particularly suited for the identification and reporting of sequential approaching events, such as an approaching vehicle with passengers desiring to breach a fenced facility. One benefit is that the likelihood of detection of intruders is increased because the sensors are designed for detection of different characteristics of an intrusion attempt. For example, if one sensor misses detection due to some confounding event, other sensors may not be susceptible to such an event, providing another chance for detection. Another benefit is that the sensors allow the system to deliver threat-level information about incoming threats. For example, vehicles detected at a long distance may have a lower threat-level than intruders approaching a secure perimeter, which in turn may have a lower threat level than the intruders attempting to scale a fence surrounding the perimeter.

The acoustic signatures of interest generated by approaching human and running vehicles are complicated. In the case

Report Documentation Page

Form Approved
OMB No. 0704-0188

1. REPORT DATE	2. REPORT TYPE	3. DATES COVERED
MAR 2011		**00-00-2011 to 00-00-2011**

4. TITLE AND SUBTITLE	5a. CONTRACT NUMBER
Intelligent Recognition Of Acoustic And Vibration Threats For Security Breach Detection, Close Proximity Danger Identification, And Perimeter Protection	5b. GRANT NUMBER
	5c. PROGRAM ELEMENT NUMBER
6. AUTHOR(S)	5d. PROJECT NUMBER
	5e. TASK NUMBER
	5f. WORK UNIT NUMBER
7. PERFORMING ORGANIZATION NAME(S) AND ADDRESS(ES) **University of Southern California,Center for Neural Engineering,Los Angeles,CA,90089**	8. PERFORMING ORGANIZATION REPORT NUMBER
9. SPONSORING/MONITORING AGENCY NAME(S) AND ADDRESS(ES)	10. SPONSOR/MONITOR'S ACRONYM(S)
	11. SPONSOR/MONITOR'S REPORT NUMBER(S)

12. DISTRIBUTION/AVAILABILITY STATEMENT
Approved for public release; distribution unlimited

13. SUPPLEMENTARY NOTES
HOMELAND SECURITY AFFAIRS, SUPPLEMENT 3 (MARCH 2011),Government or Federal Purpose Rights License

14. ABSTRACT

The protection of perimeters in national,agricultural, airport, prison, and military sites,and residential areas against dangerous approaching human and vehicles when using human agents to provide security is expensive or unsafe. Because of this, acoustic/vibration signature identification of approaching human and vehicles threats has attracted increased attention. This paper addresses the development and deployment of three types of acoustic and vibration based smart sensors to identify and report sequential approaching threats prior to the intrusion. More specifically, we have developed: a) acoustic based long range sensor with which vehicles' engine sound and type can be identified, b) vibration based seismic analyzer which discriminates between human footsteps and other seismic events such as those caused by animals, and c) fence breaching vibration sensor which can detect intentional disturbances on the fence and discriminate between climb, kick,rattle, and lean. All of these sensors were designed with several issues in mind, namely,optimized low power usage, a low number of false positives, small size, secure radio communication, and milspec. The developed vibration based system was installed in an airport with unprotected shore lines in the vicinity of taxi- and run-ways. The system reported an average of less than two false positives per week and zero false negative for the duration of forty-five days. Six fence sensors were installed on the terminal area and end-ofrunway chain-link fences where there was possibility of intentional fence climbing. The fence sensors reported no false positives for the duration of forty-five days which included several days of seasonal storms.

15. SUBJECT TERMS

16. SECURITY CLASSIFICATION OF:			17. LIMITATION OF ABSTRACT	18. NUMBER OF PAGES	19a. NAME OF RESPONSIBLE PERSON
a. REPORT **unclassified**	b. ABSTRACT **unclassified**	c. THIS PAGE **unclassified**	**Same as Report (SAR)**	**13**	

Standard Form 298 (Rev. 8-98)
Prescribed by ANSI Std Z39-18

of running vehicles, the acoustic patterns are affected by multiple factors, such as gearing, number of cylinders, muffler choice, state of maintenance, running speed, distance from the microphone, tires, the road on which the vehicle travels, and other uncontrolled environmental interference emitted by wind, bird chirp, and human voice. We propose using a neurobiology-motivated algorithm to detect approaching vehicles and to identify the type of vehicles. With the exact acoustic signature being unknown, Nonlinear Hebbian learning (NHL), a basic and appealing neural learning function found in human brain, is employed for unsupervised learning. The developed system is capable of discriminating between three types of vehicles, namely light track, heavy track, and motor cycle.

The goal of a seismic-based human threat detector is to detect approaching humans and discriminate between series of events caused by animals or passenger vehicles vs. background and a single vibration event, e.g. the falling of a tree limb. A geophone-based seismometer has been employed which is an inexpensive sensor that provides easy and instant deployment as well as long range detection capability. Gaussian mixture models were formed to model statistical properties of the temporal gait and frequency features extracted from the seismic signals. The system was set up to discriminate between human footsteps, vehicles, background (including disconnected incidents, animals' footsteps).

For the purpose of fence breach detection and classification, a 3-axis accelerometer has been utilized. The developed algorithm which is based on a nonhomogeneous Markov model is capable of recognizing the type of the breaches; whether the breach is due to the rattling caused by strong wind or a person climbing on the fence. The proposed algorithm and system has been tested on different fences and has demonstrated robust recognition for discriminating between climb, kick, rattle, and background.

METHOD

Seismic Event Recognizer: seismic discrimination between human footsteps, vehicle, and out-of-class signals.

The signal measured from a geophone has a 0.1Hz~100Hz frequency range due to the resonant characteristics of the sensors. Although the frequency response of the seismic sensor is in a narrow frequency band, spectral analysis can be used for discriminating between seismic events caused by human footsteps (or four-legged animals) and vehicles. However, due to the very similar walking mechanism of humans and animals, the generated rhythmic temporal seismic patterns of humans and animals are very similar. This renders the discrimination between a human's and an animal's footstep using frequency analysis a failure using spectral analysis alone. Therefore we propose using gait pattern analysis of seismic events to discriminate between human and animal footsteps.[2]

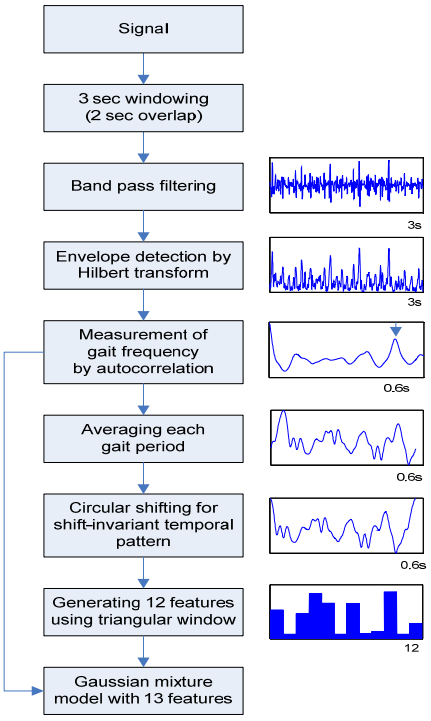

Figure 1: Feature extraction algorithm and examples of the output of each block.

The flow diagram of the method is depicted in the Figure 1. After applying a three-second sliding window – with two seconds overlap – on the incoming signal, the signal is passed through a band-pass filter to enhance the Signal to Noise Ratio (SNR). Then a Hilbert transform and low pass filtering (smoothing process) is applied to extract the envelope of the signal. In the next step, we utilize this signal to extract the mean temporal pattern of the gait by averaging over each gait periods.

Accordingly it is necessary to estimate the gait period within the three-second window and partition the three seconds signal based on gait period. This can be achieved in the following steps:

Gait period is estimated by using the auto-correlation function. Because of the periodicity in the signal, the auto-correlation signal has a local maximum at the time of gait period. In general, finding local maxima is a challenge; however, due to the resonant characteristics of the seismic sensors and the periodicity from walking mechanism, there is a detectable peak in the auto-correlation function. It also worth mentioning that the gait period (or cadence frequency) will later be employed as one of the features.

Using the estimated gait period in A, the three second window is equally divided into *k* number smaller windows each having gait period length.

The partitioned signals from B are averaged.

In order to make a shift-invariant temporal gait pattern representation, the averaged gait pattern from C is circular-shifted so that the local maximum of the pattern is on the first sample. The partitioning of the three second signal into *k* frames will have some remainder which is considered in the circular shift of the next consecutive frame.

Lastly, twelve triangular weighting functions are applied to the temporal pattern acquired from the steps explained above so that the gait temporal pattern can be represented by twelve features.

For modeling statistical variation of the extracted features, Gaussian Mixture Models (GMM) were utilized. GMM is one of the most well-known and useful classifiers, having been widely used in many applications. For a multimodal random variable, whose values are generated by one of several independent sources, a finite mixture model can be used to approximate the true probability density function. Moreover, GMM is a good candidate as a classifier when there exists no prior knowledge of a probability density function. Therefore, estimating the distribution with GMM not only provides a chance to have a general model but also helps to understand the phenomena for a better use of the information of the distribution.

A non-singular multivariate normal distribution of a *D* dimensional random variable $X \leftrightarrow x$ can be defined as:

$$X \sim N(x_c,\ \mu_c\ ,\Sigma_c) = \frac{2}{(2\pi)^D|\Sigma|^{0.5}}\ exp\left[-\frac{1}{2}\ (x - \mu)^T\Sigma^{-1}(\mathrm{x}-\mu)\right] \quad (1)$$

where μ is the mean vector and Σ the covariance matrix of the normally distributed random variable X.

The GMM can be defined as a weighted sum of Gaussians function:

$$p(x,\theta) = \sum_{c=1}^{C} \alpha_c\, N(x_c,\ \mu_c, \Sigma_c) \quad (2)$$

where α_c is the weight of c^{th} mixture and θ is defined as following.

$$\theta = \{\alpha_1,\ \mu_1, \Sigma_1, \ldots,\ \alpha_C, \mu_C, \Sigma_C\} \quad (3)$$

To estimate or train the model parameter θ, the Figueiredo-Jain (FJ) algorithm was used,[3] which automatically chooses the optimum number of mixtures during the training. The objective function of this algorithm utilizes the minimum message length criterion for finding optimum number of mixtures as defined in the equation (4) so that it can select the best model directly from data rather than the hierarchy of model-class.

$$\Lambda(\theta, x) = \frac{V}{2}\sum_{\alpha_c>0}\ln\left(\frac{N\alpha_c}{12}\right) + \frac{C_{nz}}{2}\ln\left(\frac{N}{12}\right) + \frac{C_{nz}+(V+1)}{2} - \ln\mathcal{L}(X,\theta) \quad (4)$$

where *N* is the number of training points, *V* is the number of free parameters specifying a component, and C_{nz} is the number of

mixture ($\alpha_c > 0$). The last term, $\ln\mathcal{L}(X,\theta)$, is the log-likelihood of the training data given the distribution parameters θ.

Nonhomogeneous Markov Model for fence intrusion detection and discrimination between fence climbing, rattle, kick, and background

The sensing module in the fence sensor is a 3-axis digital accelerometer (X, Y and Z axes) measuring the vibration signal acceleration range. The source of kick and lean intrusions are short-time forces imposed on the fence. As a result, the event starts with a high-level acceleration and high-frequency vibrations. As time progresses, the acceleration decays exponentially and vibration gets a harmonic structure. In climbing, rattling, and scratch intrusions, the vibration source has longer time periods. The decay pattern and the transition from high-frequency to harmonic vibration are less prominent. The intrusion signal analysis demonstrates the rattling signal to be more or less periodic, while the climb and scratch signals are chaotic.

The signal time-domain envelope plus its time-frequency features are used in intrusion classification. The time-domain envelope is represented by Z-axis energy plus relative energy in X and Y-axis to Z-axis. The time-frequency features are extracted by measuring Z and X axis signal energy in a set of filter-banks. Features are extracted in 256-point (400 ms) windows of signal with 50 percent (200 ms) overlap.

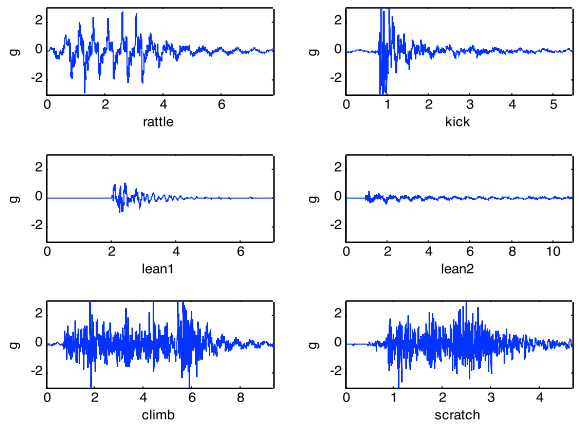

Figure 2: Z axis signal for different intrusion classes.

Intrusion signals recorded by sensors demonstrate temporal and dynamic patterns, implying the use of HMM as a standard dynamic classifier. A trivial technique for intrusion classification deals with defining and applying one HMM for each intrusion class. This method is practically inadequate, because the sensor's computational resource, a 16 MIPS RICS processor, is not sufficient for implementing five HMM models plus their post-processing task within the classifier's time resolution (200 ms, the signal update period). To go beyond this limitation, we utilized a NHMM model for intrusion localization along with a static classifier. The new classifier not only has lower computational complexity, but also presents a higher classification performance comparing to the trivial method. The chief reason for the complexity reduction plus performance improvement is the precise intrusion localization provided by NHMM. The sequence analyzer, a dynamic classifier, is designed as a 3-state HMM with a time-dependent transition probability matrix. It identifies the most probable time-window of the signal for different intrusions. Then the static classifier, a Bayesian classifier, examines the likelihood of different intrusions to find the most probable intrusion class. Data analysis shows that the performance of NHMM in intrusion localization surpasses that of homogenous HMM. Moreover, the NHMM generates higher likelihood values than HMM in signal sequences, with an equal state definition for both models. The dynamicity of transition probability matrix brings more flexibility in the model, allowing it to follow unusual and abrupt behaviors in the intrusion signal.

The logarithm of Z-axis energy in successive frames is passed to the transition probability matrix of the sequence analyzer. The energy plus time-frequency features determine the sequence observation of the analyzer. Non-intrusion (called *S1* state), harmonic (called *S2* state), and high-frequency (called *S3* state) periods determine three states of the model. In the next part, we introduce the dynamic transition probability and its training procedure.[4]

Assume $O=\{\bar{o}_i, i=1,2,\ldots,N\}$ is the observation generated by a HMM model and

its hidden states are $C = \{c_i, i = 1,2, \ldots, N\}$. The joint distribution of observation is,

$$P(O|C,\theta) = p(c_1)p(\bar{o}_1|c_1,\theta)\prod_{i=2}^{N} p(\bar{o}_i|c_i,\theta)p(c_i|c_{i-1}) \quad (1)$$

The emission process $p(\bar{o}_i|c_i, \theta)$ is considered equal for the sequence and the transition probability matrix $p(c_i|c_i\text{-}1)$ is a function of observation index, i. $\bar{o}_i$ is the feature set representing i^{th} data frame, and θ determines the state parameter. The transition matrix dependency to sequence index means that the hidden states follow a NHMM chain. To estimate parameters of the local transition probability matrix, the matrix entries are defined as a function dependent to a set of observed features.

The transition probability matrix is modeled by a function of energy in adjacent frames. Based on the state definition, the transition probability matrix, A, is a 3-by-3 matrix with the following definition for its pq^{th} entry.

$$t_{pq} = k_{pq}^1 * (e_m - e_{m-1}) + k_{pq}^2 * (e_m - e_{m-1})^2 + k_{pq}^3$$

$$a_{pq} = \frac{e^{t_{pq}}}{\sum_{q=1}^{3} e^{t_{pq}}}, A = \begin{bmatrix} a_{11} & a_{12} & a_{13} \\ a_{21} & a_{22} & a_{23} \\ a_{31} & a_{32} & a_{33} \end{bmatrix} \quad (2)$$

e_m and e_{m-1} are energy logarithms in m and $m-1$ observation frames. The A_{pq} entry, the probability of transition from state p to state q, is a soft-max function of t_{pq}, for p = {1, 2, 3} and q = {1, 2, 3}. $\{Q_p, p=1,2,3\}$ is the set of parameters defining the A matrix, in which $Q_p = \{k_{pq}^1, k_{pq}^2, k_{pq}^3, q=$. The t_{pq} is defined as quadratic function of energy logarithm's difference, representing a quadratic approximation of relative energy (e_m/ e_{m-1}) in matrix A. In fact, the energy trend in successive frames has been modeled with a second order polynomial approximation. Intuitively the k_{pq}^3 coefficient carries the homogenous part of A entries, while the k_{pq}^1 and k_{pq}^2 mutually determine the energy dependent part of A. The k_{pq}^2 magnifies energy difference in the model, while k_{pq}^1 intensifies energy trend. For example for a_{33}, we expect k_{33}^1 to be a positive number reasonably bigger than k_{33}^2. This is because in successive S3 states, energy amplitude decays by index.

The training process estimates optimized values for Q_p and Θ with maximum likelihood (ML) criteria. Each state is modeled with a multivariate Gaussian function; M_s,s={1,2,3}. The training procedure, the Baum-Welch algorithm, maximizes likelihood of the observed data by adjusting Q_p and M_s parameters. By using the logarithm of equation (2), the state and transition probability equations are factorized to additive components, making training procedure simple.

$$\begin{aligned} &\max_{Q_1,Q_2,Q_3,M_1,M_2,M_3} \log P(O|C,\theta) \\ &\propto \max_{Q_1,Q_2,Q_3,M_1,M_2,M_3}\left(\sum_{i=1}^{N}\log P(\bar{o}_i|c_i) + \sum_{i=1}^{N}\log A_{c_i c_{i-1}}(e_i,e_{i-1})\right) \\ &\propto \\ &\max_{M_1,M_2,M_3}\sum_{i=1}^{N}\log P(\bar{o}_i|c_i) + \max_{Q_1,Q_2,Q_3}\sum_{i=1}^{N}\log A_{c_i c_{i-1}}(e_i,e_{i-1}) \end{aligned} \quad (3)$$

In (3), $p(c_i|c_i\text{-}1)$ was replaced by matrix A entries and $p(c_1)$ was set to a constant number. The optimum values for θ = {M_1, M_2, M_3}, state parameters, are mean and covariance matrix of corresponding observed states. To find Q_p parameters, the second term of equation (3) can be factorized,

$$\begin{aligned} &\max_{Q_1,Q_2,Q_3}\sum_{i=1}^{N}\log A_{c_i c_{i-1}}(e_i,e_{i-1}) = \\ &\max_{Q_1,c_{i-1}\in S_1}\sum_{i=2}^{N}\log A_{c_i c_{i-1}}(e_i,e_{i-1}) + \\ &\max_{Q_2,c_{i-1}\in S_2}\sum_{i=2}^{N}\log A_{c_i c_{i-1}}(e_i,e_{i-1}) + \\ &\max_{Q_3,c_{i-1}\in S_3}\sum_{i=2}^{N}\log A_{c_i c_{i-1}}(e_i,e_{i-1}) \end{aligned} \quad (4)$$

According to (4), parameters of Q_1, Q_2, Q_3 can be optimized separately. By expanding each term of (4) using A_{pq} definition, ML estimate of the model turns to be an unconstrained optimization for corresponding Q_p parameters. The optimum parameters of Q_p can be found by gradient ascent method.

Training procedure starts with a Viterbi algorithm,[5] extracting the most probable

parameters are estimated from the decoded states. The training process repeats until the likelihood improvement of observation drops to a certain level or the decoded observation has no significant state changes. In the model definition, we assigned a specific state (S1, S2 and S3) to each part of the signal. Training signals are roughly labeled with their matching states; as a result the training initialization step starts with desired state definitions (a semi-supervised learning).

After training, the intrusion signals can be decoded with the Viterbi algorithm to localize intrusions. Figure 2 displays the extracted transition in a test signal. The recorded signal contains forty seconds of vibration in a slack fence. It contains a combination of intrusion attempts starting with two kicks and following by two leans, climbing, two scratch periods. In Figure 2, intrusion events have been localized precisely (within 200 msec of the actual event).

The localization result is passed to a state machine, a part of the sequence analyzer. The state machine determines different feature sets which are passed to the different intrusion classes of the classifier. The static classifier identifies intrusions by averaging likelihood values of two Bayesian classifiers. The first classifier's input includes time-frequency features of the signal and the second classifier processes envelope features. The classifier output is the intrusion class with maximum likelihood.

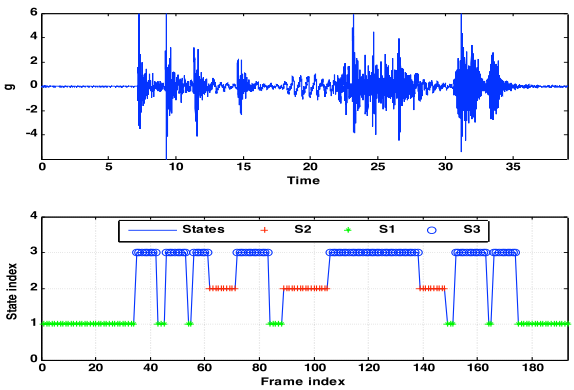

Figure 3: Top is a test signal and bottom is the output of sequence analyzer

Acoustic signature recognition of approaching vehicle using Nonlinear Hebbian Learning

The proposed approach for this research is noise-independent acoustic signature identification and recognition using spectro-temporal dynamic neural representation and Nonlinear Hebbian Learning (NHL).[6] As stated in the introduction, the acoustic sound of interest from a running vehicle is affected by multiple factors, such as gearing, number of cylinders, muffler choice, state of maintenance, running speed, distance from the microphone, tires, and the road on which the vehicle travels. As the sounds of interest from various types of vehicles may be defined by some common factors, and highly correlated between different types, vehicle type identification is also complicated because of the presence of uncontrolled interference emitted by surrounding background, such as human voice, gunshots, and wind.

The preprocessing of the proposed method mimics functions of the biological ear to correctly recognize signals of interest, even if they are noise-corrupted. The signals of interest are acoustic sounds of approaching vehicles – light track, heavy track, diesel truck, and motorcycle – which are often overlapped with environmental noises. In general these noises are highly time-varying and unknown to the recognizer. State-of-the-art feature extraction algorithms, such as Mel Frequency Cepstral Coefficients (MFCC) fail in this case, because MFCC work only in short-term spectral analysis.

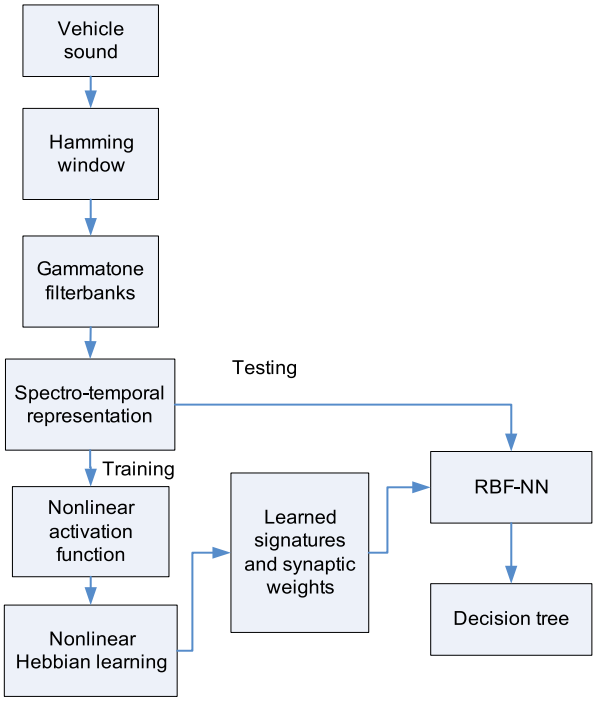

Figure 4: Flow diagram of the proposed vehicle's engine sound recognizer

As illustrated in Figure 5, the left module represents the spectro-temporal dynamic neural structure with Q frequency bins and M temporal frames. Selecting Q=30, M=20, the dimension of spectro-temporal features is 600, which may cause very complex computation at the testing stage if they are used as patterns. Besides, high-dimensional features may be less useful than real representative features as high-dimensional ones may be easily mixed with unrelated noises.

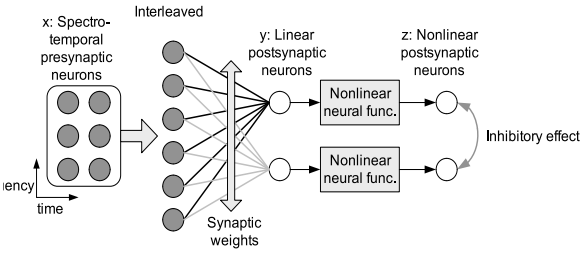

Figure 5: Nonlinear Hebbian illustration

Linear Hebbian Learning (LHL) which is equivalent to linear principal component analysis can be used for dimensionality reduction; but in an information-theoretic context, the second-order moment of LHL is inadequate to reduce data redundancy, as generally the mutual information between important components of data involves statistics of all orders. Thus, to tackle the curse of dimensionality, a NHL, an enhancement of LHL, is proposed to be capable of efficiently projecting this messy high-dimensional representation to a low-dimensional subspace. As a result, the NHL captures important features while removing unimportant ones.

NHL iteratively updates neuron outputs and synaptic weights via the following two steps. Upon convergence, representative independent features (signatures) are extracted and the projecting subspace is spanned by synaptic weight vectors.

Step I: Neuron output (signature) computation

$$Y_l = \sum_{q=1}^{Q} \sum_{m=1}^{M} w_{qml} x_{qm}, l \in [1, \dots, L] \quad (5)$$

Step II: Synaptic weight update

$$\Delta w_{qml} = \eta g(y_l) g'(y_l) \left(x_{qm} - \sum_{i=1}^{l} w_{qmi} y_i\right), \; q \in [1, \dots, Q], m \in [1, \dots, M], l \in [1, \dots, L] \quad (6)$$

where Q and M are the number of spectral bins and temporal frames, respectively. L is the number of extracted representative patterns. w_{qml} represents the connecting spectro-temporal synaptic weight from the input neuron x_{qm} to the output neuron y_1.

The nonlinear activation function $g(.)$ is the critical part in Nonlinear Hebbian Learning. If it is Taylor expanded, it can explore all order statistics of input signals and satisfy statistical optimization criterion. Moreover, this special function is derived from neurobiology studies, which supports multiple independent signal communications in response to pre-synaptic inputs.

RESULTS

The mathematical models in each technology were trained with the data recorded in a controlled environment. The recording samples for each class of intrusion were mutually exclusive from the other classes. All of the recording samples for the purpose of this study were collected in Joshua Tree, CA

for which more details can be found in the referred papers.

Two types of test were planned. The first plan was to evaluate the smart fence sensors in the Joshua Tree recording site where the training samples were collected. The second plan was to install the sensor in a completely realistic condition where the impact of environmental factors such as storm, moisture, wind, heat, and etc can also be measured. The later provides potential to observe the behavior of the sensors for unexpected incidents – such as those training samples not available during the development – and also monitor physical parameters of the sensors e.g., battery life and wireless communication issues.

Test Results in Controlled Environment

Seismic sensor

For testing seismic sensor's performance, the sensor was placed in the same site in which the training samples were recorded. During the test, the average of posteriori probabilities of each class on ten consecutive window frames was calculated (it has been assumed that there is no abrupt changes within the intrusion class). We found that the average posteriori is a powerful technique in this application which enhances the low-SNR observations results and reduces false positives.

A horse was chosen for a quadruped class because the gait can be easily controlled by a rider and also data can be easily acquired with the rider's control. The seismic sensor was tested with different types of the horse gaits, namely walk as a 4-beat gait, trot as a 2-beat gait, canter as a 3-beat gait, and gallop as a fastest 4-beat gait. In addition, the seismic sensor was also evaluated with a single person walking/running and five people walking in a group at synchronized/ unsynchronized, random speed, and random phase. Moreover, multiple vehicles with a different number of cylinders and frame size were employed to evaluate the sensor. The results of the tests are summarized in the Table 1.

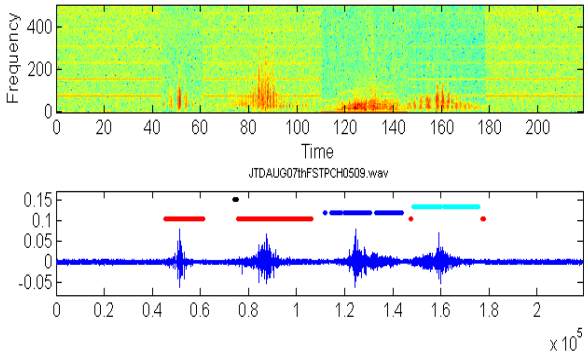

Figure 6: Bottom graph is seismic recognition of background (no bar), human footstep (red bars), dog's footstep (black bar), vehicle (blue bar), and horse (cyan bar). Top is the spectrum of the signal.

Table 1: Performance of seismic recognizer in the Joshua Tree, CA recording site; one frame is 400msec

	Background	Vehicle	Human	Quadruped
False Recog. %	0.1	0.2	3.8	1.9
Total Frames	19470	61110	26440	30380

Fence Sensor

One fence sensor was placed on a variety of fences to evaluate the performance. Fence heights ranged from 4' to 12', widths from 6' to 12', with variable tightness and looseness, variable degrees of sagging, with and without top and bottom rails, and variable diameters/ strength of holding posts.

Five male intruders were asked to disturb the fence – one at a time – and generate desired classes of intrusions. The intruders weighed from 125 to 210 pounds and demonstrated various patterns of climb and other intrusion classes. The results of the test have been summarized in the Table 2.

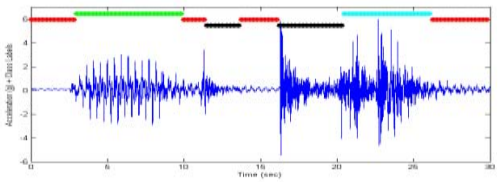

Figure 7: Recognized fence events; background (red bars), rattle (green bar), Kick (black bars), climb (cyan)

Table 2: Performance of the fence sensor evaluated on variety of fences; duration of an event can be 3 to 10 seconds depending on the type of fence and class of intrusion

	Background	Rattle	Climb	Kick
False Recog. %	0.2	0.9	1.8	2.1
Total Events	3238	2210	1045	1051

Vehicle's Engine Sound Recognizer

The proposed NHL approach was utilized to (a) recognize vehicle's engine sound and (b) detect type of engine. For the purpose of the test, light/heavy track vehicles fueled with gasoline were employed in addition to an eight cylinder diesel truck and 250cc motorcycle.

The summarized report of vehicle identification has been illustrated in the Table 3. A noise source of human speech, bird chirp, or pink noise was located next to the recording microphone in order to generate the desired signal to noise ratio.

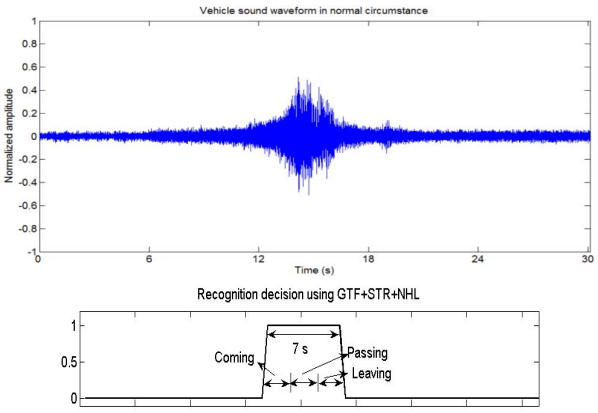

Figure 8: Top is the microphone output of a passing vehicle, and bottom is the output of the recognizer.

Table 3: Performance of vehicle identification in the Joshua Tree, CA recording site.

	Gasoline		Diesel	
SNR	Light Track	Heavy Track	Diesel Truck	Motorcycle
10 db	90%	95%	95%	100%
5 db	80%	90%	95%	95%

Test Results: Naval Surface Warfare Center's Airport Installation

The developed smart sensors were installed in an airport where some of its land is surrounded by water and there is no fence line to prevent intruders who park their boats along the shore and walk to the runway. Several footstep sensors and one vehicle engine sound recognizer were installed in front and on the roof of the boathouse respectively (see Figure 9). Moreover, several fence and footstep sensors were installed at the south end of runway where, due to its proximity to a freeway, the sensors would have the highest chance of detecting intrusions of either cars crashing into the fence and then driving into the airport or the climbing of the fence by pedestrians who could then walk into the airport. Several more fence sensors were also installed in a rental car area. A graphical user interface was developed and installed in the command center to aggregate the sensors' output and generate log and time stamp for each entry. An event-driven video recording capability was added to the smart fence functionality in order to confirm the registered alarm with the camera recordings.

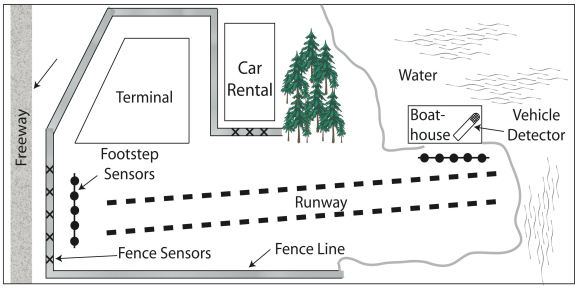

Figure 9: Blue print of the installed sensors at the airport

The efficacy of the smart fence was demonstrated in several scenarios. In the first, the approaching threat was an incoming motorboat, whose passengers disembarked on a dock located at the boundary of an airport. In the second, the threat was an incoming vehicle that drove through a rental car facility with the intention of allowing the passengers to scale a fence separating the

rental car facility from the airport tower. In the final scenario, the threats were an incoming vehicle that drove off of a major thoroughfare, with the intention of allowing the passengers to scale a fence that surrounds the end of the airport runway. Each scenario provided different conditions and threat levels. In the first, the vehicle engine sound detector detected a motorboat and the seismic analyzer detected the intruders' footsteps. In both the second and final scenarios, vehicle engine sound detection was common, but the seismic analyzer detected the intruders as they approached the fence, and the fence breaching sensor detected scaling attempts. The smart fence successfully identified the threats and generated alarms before the threats approached the secured zone.

To statistically analyze false positives, battery life, wireless issues, and environmental factors, the smart fence technology at the naval facility was monitored for a period of forty-five days. For the purpose of vehicle engine sound recognition, due to the request of authorities no test was performed therefore the forty-five days test doesn't consider the acoustic sensor. The weekly average of false positives generated by other sensors has been demonstrated in the Table 4.

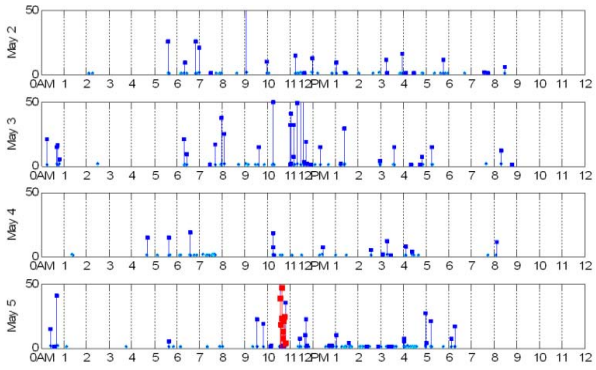

Figure 10: Daily report for one of the footstep sensors installed in front of the boathouse. Blue bars show vehicle recognition (in this care airplane either taxing or taking off), red is human footsteps; x axis is the time and y axis is the duration of an event.

Table 4: Average weekly report for the smart fence sensors

	No. of Incidents	Awake Time (min)	No. of False Positives
Fence Sensors	25	9	1.09
Footstep Sensors	1227	409	1.89

ID	Sensorid	Sensortime	Zonecontroller	Eventtype	Location
464	0000	2010/05/11 08:27:43	172.20.2.162	I	Terminal SC
465	0000	2010/05/11 08:27:43	172.20.2.162	K	Terminal SC
466	0000	2010/05/11 08:27:44	172.20.2.162	K	Terminal SC
467	0000	2010/05/11 08:27:45	172.20.2.162	K	Terminal SC
468	0000	2010/05/11 08:27:46	172.20.2.162	K	Terminal SC
469	0000	2010/05/11 08:27:47	172.20.2.162	K	Terminal SC
470	0005	2010/05/11 08:28:10	172.20.2.162	C	Terminal SC
471	0005	2010/05/11 08:28:13	172.20.2.162	C	Terminal SC
472	0005	2010/05/11 08:30:36	172.20.2.162	I	Terminal SC

Page 1 of 1 1 to 9 of 9 Records Per Page 30

Figure 11: Snapshot of a lawn mower colliding with chain-link-fence at car rental area; the sensor has generated the letter "K" as an induction of kick.

CONCLUSIONS AND FUTURE WORK

In this paper we described development of "smart fence" technology for intelligent acoustic/vibration security breach detection and recognition. The "smart fence" sensors included: (1) seismic event recognizer for human footsteps and vehicle-caused ground vibrations, (2) vibration sensor to detect intentional fence breaches and discriminate between rattle, kick, and climb, and (3) acoustic vehicle sound recognizer for

detecting an approaching vehicle and identifying type of vehicle.

The smart fence was tested in controlled and uncontrolled environments. In the controlled environment the threat seismic event recognizer showed above 98% performance and the average performance was more than 98% and 97% for the fence and vehicle's engine sound recognizers. The uncontrolled and forty-five days test of the sensors proved that all sensors have extremely low false positives. Also, the test coinciding with the local storm season provided opportunities to measure the performance of the recognizers in the presence of extreme weather conditions such as heavy rain and wind. Indubitably, wind and rain can have significant impact on sound and vibrations. However, as the average weekly report summarized in the Table 4 demonstrates, the extreme weather conditions have not generated a challenge to the sensors' performance.

During both controlled and uncontrolled tests we observed that the seismic sensors perform close to ideal when the threat is in the radius of sixty feet. We also found that for each panel of chain-link fence there is a need for one sensor regardless of width and height of the fence. The reliable detection range for the vehicle engine sound recognizer was 120 feet direct line-of-sight. These findings suggest that the manufacturing cost of each technology should be very cheap – and easy to install and maintain – for the purpose of protecting a several-mile-long perimeter of an airport. All of the designed technologies have satisfied the low cost condition.

Security breaches often follow certain sequences. As an example, an intruder must take a few steps before disturbing the fence. A false fence disturbance detection by a fence sensor due to the wind can be eliminated if the output of the seismic sensor is combined with the fence recognizer. High-level data fusing of the sensors of this study not only could enhance the false positives and true negatives, it could also provide management of the threats by airport authorities. Sequential modeling and analysis of detected threat by smart fence sensors is the plan for the future work.

ABOUT THE AUTHORS

Theodore W. Berger, PhD, is the David Packard Professor of Engineering, Professor of Biomedical Engineering and Neuroscience, and Director of the Center for Neural Engineering at the University of Southern California.

Alireza A. Dibazar, PhD, is assistant professor of computational neural engineering and co-director of the USC Laboratory for Neural Dynamics. Dr. Dibazar is actively involved in many scientific organizations such as IEEE, IEE, SFN, JASA, EMBC, and BMES. He may be contacted at dibazar@usc.edu.

Bing Lu received her PhD from the Department of Biomedical Engineering at the University of Southern California in 2009. Her research areas are pattern recognition, neural networks,artificial intelligence, and computer vision.

Hyung O. Park received his PhD in Biomedical Engineering Aug 2010 from the University of Southern California. He is currently with USC's Laboratory for Neural Dynamics (LND).

Ali Yousefi is a PhD candidate at the University of Southern California Electrical Engineering Department. He is working in the Neural Dynamics Laboratory under supervision of Professor Alireza Dibazar and Theodore Berger.

[1] This research was supported by the awards from ONR (award #N00014-10-1-0685) and the Navy through a CPP grant (award #N00014-09-C-0209).

[2] H. O. park, A. A. Dibazar, and T. W. Berger, "Cadence Analysis of Temporal Gait Patterns for Seismic Discrimination Between Human and Quadruped Footsteps," *Proceedings of the ICASSP* (2009): 1749-1752.

[3] M. Figueiredo and A. Jain, "Unsupervised learning of finite mixture models," *IEEE Trans. Pattern Anal. Machine Intell.* 24, no. 3 (2002): 381–396.

[4] A. Yousefi, A. A. Dibazar, and T. W. Berger, "Application of Non-homogenious HMM on Detecting Security Fence Breaching," *Proceedings of the ICASSP* (2010).

[5] L. Rabiner and B. Juang, "An Introduction to Hidden Markov Models," *ASSP Magazine* 3, no. 1 (IEEE: January 1986): 4-16.

[6] B. Lu, A. Dibazar, and T. W. Berger, "Perimeter Security on Detecting Acoustic Signature of Approaching Vehicle Using Nonlinear Neural Computation," *Proceedings of the IEEE Technologies for Homeland Security* (2008): 1122-1125.